ELSEVIER

Theoretical analysis of femtosecond excitation and fragmentation dynamics of Fe(CO)$_5$

O. Rubner [a], T. Baumert [b], M. Bergt [c], B. Kiefer [c], G. Gerber [c], V. Engel [a,*]

[a] *Institut für Physikalische Chemie, Universität Würzburg, Am Hubland, D-97074 Würzburg, Germany*
[b] *Fachbereich Physik, Universität Kassel, Heinrich-Plett-Straße 40, D-34121 Kassel, Germany*
[c] *Physikalisches Institut, Universität Würzburg, Am Hubland, D-97074 Würzburg, Germany*

Abstract

We present the application of a time-dependent model to Fe(CO)$_5$ dissociation after femtosecond excitation to understand transient signals obtained in recent pump/probe experiments. The calculation of time-dependent energy distributions allows us to interpret the decay behaviour of the various fragments. The results indicate that at least two dissociation pathways have to be considered to explain the transient signals obtained for the different fragments. Furthermore, it is shown that, within each of the pathways discussed, concerted and sequential fragmentation compete. © 2000 Elsevier Science B.V. All rights reserved.

1. Introduction

Femtosecond time-resolved experiments are able to monitor molecular motion in real time [1–4]. This, in particular, applies to photochemical fragmentation processes. In fact, the first gas-phase experiment with femtosecond resolution examined the breaking of a chemical bond in the ICN molecule [5,6]. Recently, several femtosecond studies of the breaking of metal–ligand bonds were reported [7–15]. A system which was extensively studied using cw-laser sources is the Fe(CO)$_5$ molecule (see, e.g., Refs. [16,17]). Zewail and co-workers performed ultrafast electron diffraction (UED) experiments on this molecule [18] and, in experiments performed in our laboratory, the first femtosecond transients were obtained [14,15]. The latter results indicated that the dissociation after multiphoton excitation takes place on a timescale much shorter than one picosecond and evidence was found to support a partially concerted decay.

The complicated electronic structure of excited states in organometallic molecules [19] restricts a fully ab initio treatment where one first calculates potential energy surfaces and couplings between them, and, in a second step, performs dynamical calculations using the potentials as an input [20]. Although several quantum-chemical studies on excited states of Fe(CO)$_5$ have been reported [21,22], the goal to obtain potentials as a function of selected relevant nuclear coordinates is far from being achieved.

In the present Letter, we take a different approach to treat the photochemistry of iron pentacarbonyl. Therefore, we set up a time-dependent model based

---

* Corresponding author. Tel.: +49-931-888-6376; fax: +49-931-888-6378; e-mail: voen@phys-chemie.uni-wuerzburg.de

on ideas of quantum-mechanical perturbation theory and transition probabilities. A similar, although simpler, approach was used before [23] to describe successfully the UED experiments of Ihee et al. [18].

After giving a brief description of our experiments (Section 2), the basic ingredients of the theory are summarized in Section 3, Section 4 contains the results for the time-resolved spectroscopy of $Fe(CO)_5$. Finally, a summary and outlook are given in Section 5.

2. Experiment

The experimental setup has been described in detail elsewhere [14,15] and only a brief description will be given here. In the experiments, we employed a Ti:Sapphire chirped-pulse amplification (CPA) laser system providing 80 fs, 1 mJ laser pulses at 800 nm and at a repetition rate of 1 kHz. After second harmonic generation, the 400 and 800 nm laser beams are separated by means of a dichroic mirror. The probe laser pulses (800 nm) are delayed with respect to the pump laser pulses (400 nm) using a computer-controlled Mach–Zehnder interferometer. Both laser beams are recombined using a dichroic mirror and focused with a 300 mm quartz lens into a molecular beam of $Fe(CO)_5$ (98%; Stream Chemicals), which is taken directly from the cylinder at room temperature (vapor pressure of ≈ 40 Torr) and expanded through a nozzle of 50 μm. The ionic photoproducts are detected with a time-of-flight (TOF) mass spectrometer. The transient ionization spectra measured by means of boxcar integrators were averaged to obtain a sufficient signal-to-noise ratio.

All transient spectra were recorded with attenuated pump- and probe-laser beams so that the observed dynamics has to occur in the neutral molecule (for details see Refs. [14,15]).

3. Theory

3.1. Time-dependent model

In this section, we outline our model which is used to describe the $Fe(CO)_5$ fragmentation dynam-

ics. An iterative scheme which calculates the internal energy distributions $g_n(E_n, t)$ of the $Fe(CO)_n$ ($n = 0$–5) molecules is employed. The latter give the probability to find a fragment with n CO ligands with energy E_n at time t. Starting with an m-photon excitation of the parent molecule, the energy distribution at time $t + \Delta t$ (Δt being the time step) is given as

$$g_5(E_5, t + \Delta t)$$
$$= |\langle E_5 | \psi^{(m)}(E_5, t + \Delta t) \rangle|^2$$
$$+ \int dE_4 \; g_5(E_5, t) e^{-k_5(E_5)\Delta t} \; P(E_5, E_4). \quad (1)$$

Here $\langle E_5 | \psi^{(m)}(t + \Delta t) \rangle$ is the projection of the state $|\psi^{(m)}(t + \Delta t)\rangle$ of $Fe(CO)_5$, prepared by a laser–molecule interaction during the time-interval Δt, on the energy eigenstate $|E_5\rangle$. Within a wavepacket picture, a linear combination of such states is prepared. The corresponding coordinate-space wavefunction moves on the multidimensional potential energy surface of $Fe(CO)_5$ in a region where the molecule can still be regarded as bound. However, in the course of time parts of the wavepacket will reach the $Fe(CO)_4$ + CO reaction channel so that the population in the parent molecule decreases. Since details of this coherent wavepacket dynamics are not accessible (see the discussion in Section 1), we assume an exponential decay with a constant $k_5(E_5)$ weighted with $P(E_5, E_4)$ which is the probability for the decay from an initial state with energy E_5 to a fragment state of energy E_4. The interpretation of Eq. (1) is as follows: the first term describes the increase of population prepared by the laser excitation process during Δt. The second term represents the remaining population after the fragmentation into all accessible states. We note that the above assumptions do not assume any statistical redistribution of energy and that excitation as well as fragmentation processes are perfectly coherent.

The next dissociation step is treated in a similar way leading to the expression

$$g_4(E_4, t + \Delta t)$$
$$= \int dE_5 \; g_5(E_5, t)(1 - e^{-k_5(E_5)\Delta t}) \; P(E_5, E_4)$$
$$+ \int dE_3 \; g_4(E_4, t) e^{-k_4(E_4)\Delta t} \; P(E_4, E_3), \quad (2)$$

where the different quantities have the same meaning as described above. Here the first term describes the increase of population due to the decay of $Fe(CO)_5$ and the second term describes the decrease due to further dissociation. All other fragmentation steps are treated in a similar way.

The knowledge of the energy distributions g_n allows for a calculation of the populations $S_n(t)$ which measure the amount of molecules $Fe(CO)_n$ found at time t:

$$S_n(t) = \int_0^\infty dE_n \, g_n(E_n, t). \tag{3}$$

Note that, if the lower integration limit is set to the threshold energy for dissociation E_{thr}, the integral counts the fraction of molecules which are able to undergo further fragmentation.

The above scheme describes a sequential dissociation; see, however, the discussion concerning concerted decay processes in Section 3.2 Several quantities enter in a numerical evaluation of the expressions. $|\psi^{(m)}(t + \Delta t)\rangle$ can be evaluated within perturbation theory as (atomic units are used)

$$|\psi^{(m)}(t + \Delta t)\rangle = \frac{1}{i} \, W(t + \Delta t) \, |\psi^{(m-1)}(t)\rangle, \tag{4}$$

where W denotes the molecule–field interaction energy and $|\psi^{(m-1)}(t)\rangle$ is the wavefunction obtained by an absorption of $(m-1)$ photons.

Next, the rate constants $k_n(E_n)$ have to be specified using one or the other model. Finally, one has to define an explicit form of the transition probabilities $P(E_n, E_{n-1})$.

3.2. Application to $Fe(CO)_5$

We will now apply our model to the laser-induced fragmentation dynamics of $Fe(CO)_5$. Fig. 1 shows the threshold energies for the dissociation into the various reaction channels producing fragments in the ground electronic state [21]. Also, energies corresponding to the absorption of one, two and three photons at 400 nm (3.1 eV) are shown in the figure. For the absorption of a single photon, not all fragment channels are energetically open so that this process will not be treated in what follows [15]. In Section 4, we discuss the fragmentation processes
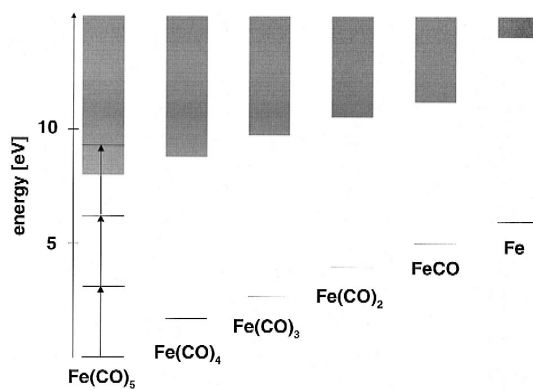

Fig. 1. Threshold energies for $Fe(CO)_5$ dissociation into the electronic ground state of smaller fragments. The arrows indicate the photon energy of 3.1 eV (corresponding to the 400 nm excitation pulse in the experiment). The shaded areas indicate the respective ionization continua.

initiated by absorption of two and three photons separately.

A proper description of the pump-excitation process involves the determination of the states $|\psi^{(m)}(t)\rangle$ with $m = 1, 2, 3$. Let us discuss a three-photon resonant excitation. In this case, we represent the Hamiltonian of the unperturbed parent molecule as

$$H_0 = \sum{}' \{|E_5'\rangle \, E_5' \, \langle E_5'|\} + |\varepsilon_2\rangle \, \varepsilon_2 \, \langle \varepsilon_2| + |\varepsilon_1\rangle$$
$$\times \varepsilon_1 \, \langle \varepsilon_1| + |\varepsilon_0\rangle \, \varepsilon_0 \, \langle \varepsilon_0|. \tag{5}$$

The sum extends over the discretized continuum of final states $|E_5'\rangle$ and $|\varepsilon_n\rangle$ are the initial ($n = 0$) and intermediate ($n = 2, 3$), resonantly excited states. The energies of the intermediate states are marked in Fig. 1. They correspond to multiples of the laser carrier frequency ω which, in our case, has a photon energy of 3.1 eV.

The interaction is written as

$$W(t) = -\frac{1}{2} f(t) \, e^{-i\omega t} \{|E_5\rangle \, \mu \, \langle \varepsilon_2| + |\varepsilon_2\rangle$$
$$\times \mu \, \langle \varepsilon_1| + |\varepsilon_1\rangle \, \mu \, \langle \varepsilon_0|\}, \tag{6}$$

where $f(t)$ is a pulse envelope and μ are transition-dipole moment elements. The numerical calculations use Gaussian envelope functions with a temporal width (full width at half maximum) of 80 fs.

The amplitude for the preparation of a state via a three-photon transition is obtained by projection of $|\psi^{(3)}(t)\rangle$ on $\langle E_5|$ to obtain

$$
\begin{aligned}
&\langle E_5|\psi^{(3)}(t)\rangle \\
&= \left(\frac{-1}{2i}\right)^3 \int_{-\infty}^{t} dt' \int_{-\infty}^{t'} dt'' \int_{-\infty}^{t''} dt''' \\
&\quad \times \langle E_5|\mu|\varepsilon_2\rangle\langle\varepsilon_2|\mu|\varepsilon_1\rangle\langle\varepsilon_1|\mu|\varepsilon_0\rangle \\
&\quad \times f(t')\, f(t'')\, f(t''')\, e^{-i\omega(t'+t''+t''')} \\
&\quad \times e^{-iE_K(t-t')}\, e^{-i\varepsilon_2(t'-t'')}\, e^{-i\varepsilon_1(t''-t''')}\, e^{-i\varepsilon_0 t'''} .
\end{aligned}
\tag{7}
$$

In the calculation, all matrix elements appearing in (7) are set to unity. The remaining time integrals are evaluated iteratively [24]. Within this model, the energy distribution $|\langle E_5|\psi^{(3)}(t)\rangle|^2$ resembles a Gaussian peaked around an energy $E_5 = 3 \times 3.1$ eV.

For the $Fe(CO)_5 \rightarrow Fe(CO)_4$ step, we assume a direct dissociation on an exponentially decaying potential ($V(x) = V_0 e^{-\alpha x}$) along the reaction coordinate x. The rate constant is estimated as the inverse of the time, a classical particle (or the center of the quantum-mechanical wavepacket) with the reduced mass μ of $Fe(CO)_4 + CO$ needs to reach a critical distance ℓ where the bond is assumed to be broken, starting at $x = 0$ with zero momentum. As an analytical result one obtains:

$$
k_5 = \sqrt{\frac{V_0 \alpha^2}{2\mu}} \, \frac{1}{\mathrm{arcosh}(e^{(\alpha/2)\ell})} .
\tag{8}
$$

We assume that V_0 equals the energy of $Fe(CO)_5$ above the dissociation threshold; thus k_5 scales with the square root of this energy. In all calculations we used $\ell = 5$ Å and $\alpha = 1$ Å^{-1}. The value for ℓ corresponds to about three times the Fe–C distance in $Fe(CO)_5$ and thus is not unreasonable.

Following experimental evidence [15], we assume the subsequent dissociation processes to occur in an indirect way. The harmonic Slater model [25,26] is employed to calculate the respective rate constants. Within this model, the time dependence of a Fe–C bond distance $x_n(E_n,t)$ in a fragment $Fe(CO)_n$ with energy E_n is given as:

$$
x_n(E_n,t) = \sum_{j=1}^{s_n} \alpha_{nj}\, \chi_{nj}^0\, \cos(\omega_{nj} t),
\tag{9}
$$

with

$$
\chi_{nj}^0 = \sqrt{\frac{2\varepsilon_{nj}}{\omega_{nj}^2}} .
\tag{10}
$$

ε_{nj} denotes the energy disposed in the normal mode (nj) with frequency ω_{nj} and s_n is the total number of modes. We assume that the available energy is distributed equally into the normal modes. The relative phases were set to zero as they are of no importance in what follows. The factors α_{nj} are the coefficients of the coordinate x_n when expanded in normal modes. Within this model, the dissociation constant is given by the frequency of $x_{nj}(E_n,t)$ reaching the critical distance ℓ. The latter can be determined numerically by finding the zeros of the function $f_n(E_n,t) = x_n(E_n,t) - \ell$. In more detail, we calculate $f_n(E_n,t)$ for each fragment and a selected number of relevant energies. Since this function is periodic with period $T_n(E_n)$, the numbers of zeros $m(n)$ within one period is determined and the rate constant then is $k_n(E_n) = m(n)/T_n$.

Let us make the connection to the wavepacket picture for this indirect dissociation process. A wavepacket in any of the fragments performs a time-dependent bound-state motion in all degrees of freedom except the one corresponding to the dissociation coordinate. The Slater model estimates the time it takes, in the average, for parts of the wavepacket to pass the critical distance for dissociation in the reaction channel. Since there is no loss of coherence during this motion, experiments can be performed exerting coherent control of the dissociation process [27].

We note that, within this model for indirect dissociation, it is possible to distinguish between a sequential and a concerted dissociation. Regard, e.g., the $Fe(CO)_4$ fragment produced by the fragmentation of $Fe(CO)_5$. There is a certain probability that one (or more) of the Fe–C bonds of the newly formed molecule is already elongated beyond the critical distance ℓ. In the wavepacket picture this is equivalent to a situation where parts of the prepared wavepacket are localized not only in one dissociation channel but in two or even more of them. In order to calculate this probability, we use the following ansatz. From the function $f_4(E_4,t)$, we are able to

calculate the length $\tau_4(E_4)$ of the time intervals within the period T_4 for which $f_4 > 0$. Then, the probability that one bond in $Fe(CO)_4$ exceeds the critical distance ℓ is given by $s_4 = \tau_4/T_4$. Accordingly, a fraction of molecules (equal to $g_4(E_4) \times s_4$) already dissociated into $Fe(CO)_3 + CO$. Thus the ratio of sequential versus concerted decay is given as $\wp_4 = s_4/(1 - s_4)$. Within our iteration scheme, the number of already decayed $Fe(CO)_4$ molecules has to be subtracted from $g_4(E_4, t)$ and added to $g_3(E_3, t)$. The same procedure can also be applied to the smaller fragments. Note that, even though we have to calculate this kind of decay in a sequential way, i.e. first the amount of $Fe(CO)_4$ which has a bond stretched beyond ℓ then that one of $Fe(FO)_3$ and so on, this scheme describes a concerted dissociation because all of this happens within one timestep.

The probabilities $P(E_n, E_{n-1})$ are assumed to be proportional to the density of fragment states:

$$P(E_n, E_{n-1}) = \rho_{n-1}(E_{n-1}) \, \rho_{CO}(E_n - E_{n-1}),$$
(11)

where proper normalization is assumed. The densities of states are calculated using the Whitten–Rabinovitch formula [28,29] using data from Ref. [30]. As there is almost no data for the vibrational frequencies of all the states which we have to consider, we used the values of the ground state of $Fe(CO)_5$ for the excited states of the iron carbonyls and the ground states of the fragments.

4. Results

In simulating our pump–probe transient signals, one should keep in mind that the model described in the last section is only able to describe fragmentation processes within the manifold of neutral states. Assuming that the ionization step directly probes the populations of neutral $Fe(CO)_n$ fragments, we identify the pump–probe signals with the populations $S_n(t)$, as given in Eq. (3).

Fig. 2 compares the experimental signals with the calculated populations for two-photon (dashed line) and three-photon (solid line) excitation. The simulations are restricted to positive delay times. Also, the
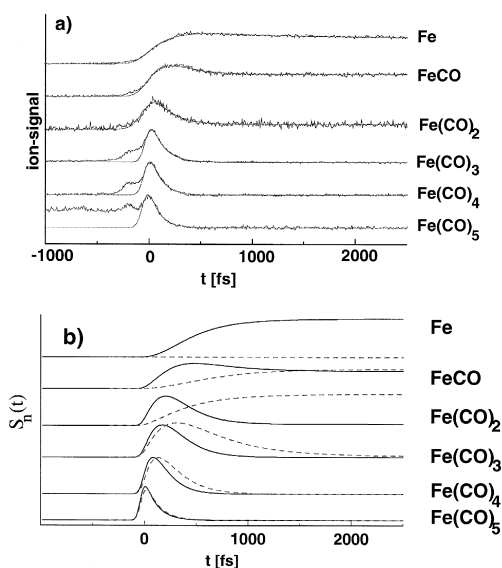

Fig. 2. (a) Measured ion signals as a function of pump–probe delay. (b) Calculated populations S_n for two-photon (dashed line) and three-photon (solid line) absorption from the pump pulse.

theoretical curves for the single fragments are not drawn on the same scale in order to facilitate the comparison with experiment. We note that the model is not able to predict the ratios of ion signals from different fragments since only the neutral manifold of molecules is described.

All measured transients were fitted using a non-linear least-square method based on a Marquardt–Levenberg algorithm where the corresponding molecular response function (single or multiple-exponential with rise and decay components) was convoluted with a Gaussian whose width (FWHM) corresponds to the cross-correlation (120 fs, determined by sum frequency mixing in a 0.1 mm BBO crystal) of the laser pulses. The parent mass transient and the transients of the fragments $Fe(CO)_4$ and $Fe(CO)_3$ were fitted to single exponentials with decay times of 100 ± 5 fs, 105 ± 5 fs and 115 ± 5 fs, respectively. The $Fe(CO)_2$ transient consists of an unresolved rise time (< 20 fs) and a decay time of 150 ± 20 fs with an asymptotic level, which is time independent for more than 100 ps. The $Fe(CO)$ transient was fitted with a rise time of 120 ± 20 fs and a decay time of 230 ± 20 fs. The transient of the atomic Fe fragment was fitted to an exponential rise
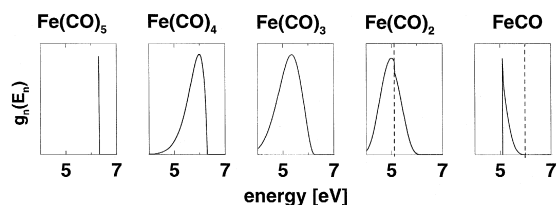
Fig. 3. Normalized energy distributions $g_n(E_n,t)$ of the molecules Fe(CO)$_n$ at $t = 250$ fs. The dashed lines indicate the dissociation threshold (see also Fig. 1).

with a time constant of 260 ± 20 fs, and an exponential decay with a time constant of 490 ± 50 fs.

Let us first discuss the two-photon dissociation pathway. The transients for Fe(CO)$_5$ and Fe(CO)$_4$ compare well to the experimental results. A different behaviour is found for the smaller fragments. In particular, the calculations predict a monotonous increase for Fe(CO)$_2$ and FeCO. Even more dramatically, within theory no atomic iron is produced in the dissociation process. Whereas this can be understood within the model (see below) this is in sharp contrast to the experimental findings. Therefore we conclude that the two-photon initiated multiple fragmentation process is not the only one leading to the manifold of fragments.

To get more insight into the fragmentation dynamics as predicted by theory, we show the energy distributions $g_n(E_n,t)$ in Fig. 3 for $t = 250$ fs. The curves are normalized to the same value at their respective maximum. We note that only the intensity but not the form of the functions depend on time.

In the beginning, the energy distribution of Fe(CO)$_5$ reflects the Gaussian shape of the excitation pulse (not visible on the present scale). In the course of the dissociation, this distribution becomes wider and shifts to lower energies. Then, in the fragment Fe(CO)$_2$, the dissociation threshold (indicated as a dashed line) is reached by a fraction of the molecules so that only those with energy above E_{thr} can dissociate. FeCO molecules are exclusively built with energies below the dissociation threshold; hence they cannot dissociate. The energy shift of the distributions in going from one fragment to the next is due to the distribution of the total energy into the Fe(CO)$_n$ and CO. Here the model predicts that about 0.5 eV of the maximal energy of a parent molecule is transferred to a dissociating CO. The shift influences

the timescale for dissociation which can be understood from the energy-dependence of the rate constants $k_n(E_n)$. The latter are shown in Fig. 4 together with the functions $g_n(E_n,t)$ for $t = 250$ fs. Only the indirect dissociation processes are considered. It can be taken from the figure that Fe(CO)$_3$ decays with a smaller average rate constant than Fe(CO)$_4$, consistent with the calculated transients displayed in Fig. 2b.

Fig. 2b also contains the calculated transients for an initial excitation with three photons. From Fig. 1, it is evident that the absorbed energy is high enough to ionize the parent molecule. Since our model treats only neutral species, we assume that an excited neutral state is prepared where the lifetime for autoionization is long enough so that neutral fragmentation occurs first. We note that an absorption band of Fe(CO)$_5$ was characterized experimentally in the range of 8–11 eV and several electronically excited states of the neutral molecule were identified [22]. Also, there is the possibility that the smaller fragments which are produced via a two-photon excitation already during the interaction of the pump pulse with the sample, might absorb another photon to build higher excited neutral molecules.

Because of the high excess energy, the distributions $g_n(E_n,t)$ are now shifted towards larger energies compared to the ones shown in Fig. 4. This
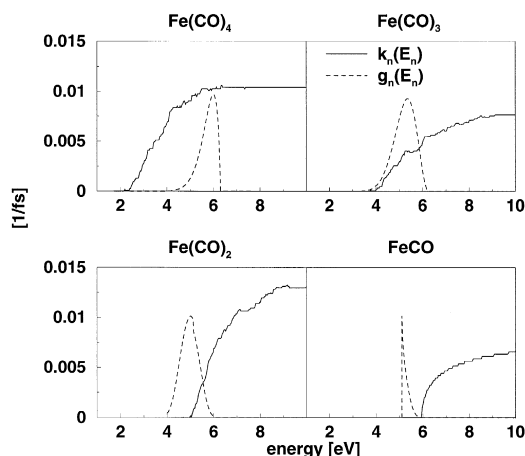

Fig. 4. Energy-dependent rate constants $k_n(E_n)$ for the unimolecular decay of Fe(CO)$_n$, ($n = 1$–4), calculated within the harmonic Slater model for indirect decay. Also shown are the (normalized) energy distributions $g_n(E_n, t = 250$ fs) (dashed lines).

results in a faster decay of the various fragments. Furthermore, now the $Fe(CO)_2$ molecules possess enough energy to dissociate. For FeCO, the threshold is reached so that only about 60% of the molecules are able to dissociate. Thus an increasing transient for atomic iron is found.

Taking the two- as well as the three-photon processes into account, it is possible to achieve excellent agreement between theory and experiment. Within the model, we find that the transients for $Fe(CO)_5$ and $Fe(CO)_4$ have a similar time dependence for both mechanisms. Whereas $Fe(CO)_3$ represents an intermediate case, the $Fe(CO)_2$, FeCO and Fe transients are predicted to be dominated by the three-photon dissociation pathway.

Let us now turn to the question of competing sequential versus concerted dissociation. As outlined in Section 3.2, the percentage of molecules which decay in a concerted way can be estimated within our model. For the three-photon process, we find that about 35–45% of the $Fe(CO)_n$ ($n = 2$–4) molecules dissociate immediately into smaller fragments whereas in the case of FeCO the fraction is only 7%. In the two-photon case, the numbers vary between 15% ($Fe(CO)_2$) and 40% for $Fe(CO)_4$.

5. Summary

We presented a model to describe the short-pulse excitation and following decay dynamics of iron pentacarbonyl. Therefore, the initial excitation step is treated using quantum-mechanical perturbation theory. The fragmentation may occur in a direct or indirect way and the respective energy-dependent rate constants are calculated assuming a direct initial dissociation step and subsequent indirect processes. In this way, we obtain the population in all energetically accessible fragmentation channels as a function of time. The model uses only two parameters, namely the critical distance where an Fe–CO bond can be regarded as broken and the steepness of the exponential potential which describes the initial direct decay of $Fe(CO)_5$.

Two- and three-photon initiated fragmentation processes were treated separately. The theoretically obtained transients for $Fe(CO)_5$ and $Fe(CO)_4$ agree well with experiment for both pathways. However, the model predicts that the two-photon process alone cannot account for the time behaviour of the signals for the smaller fragments. In particular, no atomic iron is built. On the other hand, the results for the three-photon fragmentation pathway can reproduce the transients for the smaller fragments. This suggests that (besides other processes taking part in the neutral and ionic manifold of electronic states) different multiphoton processes are likely to participate in the complicated excitation and fragmentation dynamics of $Fe(CO)_5$.

The calculations assumed that the initial fragmentation step of $Fe(CO)_5$ into $Fe(CO)_4$ and CO proceeds directly, whereas the following dissociations take place in an indirect way. The good agreement with experiment shows that this assumption is not unreasonable. Within our model, we estimate that, dependent on the fragment size and the fragmentation pathway, about 15–45% of the parent molecules directly dissociate into smaller fragments so that sequential and concerted dissociation compete with each other.

The results encourage us to apply the model to similar systems. Simultaneously an extension to take the probe process properly into account will be made.

References

[1] A.H. Zewail, Femtochemistry World Scientific, Singapore, 1994.
[2] J. Manz, L. Wöste (Eds.), Femtosecond Chemistry, VCH, Weinheim, 1995.
[3] M. Chergui (Ed.), Femtochemistry, World Scientific, Singapore, 1996.
[4] V. Sundström (Ed.), Femtochemistry and Femtobiology, Imperial College Press, London, 1997.
[5] M. Dantus, M.J. Rosker, A.H. Zewail, J. Chem. Phys. 87 (1987) 2395.
[6] M.J. Rosker, M. Dantus, A.H. Zewail, Science 241 (1988) 1200.

[7] S.A. Angel, P.A. Hansen, E.J. Heilweil, J.C. Stephenson, in: C. B Harris, E.P. Ippen, G.A. Mourou, A.H. Zewail (Eds.), Ultrafast Phenomena VII, Springer Series in Chemical Physics, vol. 53, Springer, Berlin, 1990, p. 480.

[8] S.K. Kim, S. Pedersen, A.H. Zewail, Chem. Phys. Lett. 233 (1995) 500.

[9] T. Lian, W.E. Bromberg, M.C. Asplund, H. Yang, C.B. Harris, J. Phys. Chem. 100 (1996) 11994.

[10] S.A. Trushin, W. Fuß, W.E. Schmid, K.L. Kompa, J. Phys. Chem. A 102 (1998) 4129.

[11] S.A. Trushin, W. Fuß, K.L. Kompa, W.E. Schmid, J. Phys. Chem. A (submitted).

[12] M. Gutmann, J.M. Janello, M.S. Dickebohm, M. Grossekathoefer, J. Lindener-Roenneke, J. Phys. Chem. A 102 (1998) 4138.

[13] M. Gutmann, J.M. Janello, M.S. Dickebohm, Chem. Phys. 239 (1998) 317.

[14] L. Bañares, T. Baumert, M. Bergt, B. Kiefer, G. Gerber, Chem. Phys. Lett. 267 (1997) 141.

[15] L. Bañares, T. Baumert, M. Bergt, B. Kiefer, G. Gerber, J. Chem. Phys. 108 (1997) 5799.

[16] I.M. Waller, J.W. Hepburn, J. Chem. Phys. 88 (1988) 6658.

[17] R.J. Ryther, E. Weitz, J. Phys. Chem. 96 (1992) 2561.

[18] H. Ihee, J. Cao, A.H. Zewail, Chem. Phys. Lett. 281 (1997) 10.

[19] A. Veillard (Ed.), Quantum Chemistry: The Challenge of Transition Metals and Coordination Chemistry, NATO ASI Series C, vol. 176, Reidel Publ., Dordrecht, 1986.

[20] R. Schinke, Photodissociation Dynamics, Cambridge University Press, Cambridge, 1993.

[21] L.A. Barnes, M. Rosi, C.W. Bauchschlicher, J. Chem. Phys. 94 (1991) 2031.

[22] A. Marquez, C. Daniel, J.F. Sanz, J. Phys. Chem. 96 (1992) 121.

[23] O. Rubner, V. Engel, C. Daniel, Chem. Phys. Lett. 293 (1998) 485.

[24] C. Meier, V. Engel, in: J. Manz, L. Wöste (Eds.), Femtosecond Chemistry, VCH, Weinheim, 1995, Ch. 11.

[25] N.B. Slater, Proc. Camb. Phil. Soc. 35 (1939) 56.

[26] K.A. Holbrook, M.J. Pilling, S.H. Robertson, Unimolecular Reactions, 2nd edn., Wiley, New York, 1996.

[27] M. Bergt, T. Brixner, B. Kiefer, M. Strehle, G. Gerber, J. Phys. Chem., submitted.

[28] G.Z. Whitten, B.S. Rabinovitch, J. Chem. Phys. 38 (1963) 2466.

[29] G.Z. Whitten, B.S. Rabinovitch, J. Chem. Phys. 41 (1964) 1883.

[30] W.F.T. Pistorius, P.C. Haarhoff, J. Chem. Phys. 31 (1959) 1439.